ISSN: 2414-1895 DOI: 10.6919/ICJE.202405_10(5).0057

Experimental Study on Mechanical Properties of Wood-steel Composite I-beams with Small Shear Span Ratio

Hanbing Hu[a], Xiaoxiong Liu[b]

College of civil engineer, Central South University of Forestry and Technology, Changsha 410004, China

[a]hu18753047588@163.com, [b]17763604883@163.com

Abstract

Compared with traditional steel-concrete composite beams, bolted wood-steel composite beams have advantages of short on-site installation period and light self-weight, showing promising application prospects. However, research on the mechanical properties of wood-steel composite beams is still limited. In order to investigate the influence of the ratio of wood board thickness to steel I-beam height (referred to as thickness-to-height ratio) on the mechanical properties of wood-steel composite I-beams with small shear span ratio, three groups of four wood-steel composite I-beams were designed by changing the wood board thickness while keeping the total height of the beam section, beam length, and shear span ratio at 2 constant. Bearing capacity failure tests were conducted, obtaining the failure modes, failure mechanisms, load-displacement relationships, and load-slip responses of the test beams. The experimental results indicate that all three groups of wood-steel composite I-beams ultimately failed in a bending failure mode caused by tensile failure of the flange wood boards. Meanwhile, different degrees of longitudinal splitting of the flange boards and local buckling of the flanges of the steel I-beams occurred in all three groups of specimens. This is because the shear resistance of the steel web is high, and shear failure did not occur, so an increase in the thickness-to-height ratio does not affect the failure mode. As the thickness-to-height ratio increases, the ultimate bearing capacity of the composite beams decreases, the safety factor decreases, the entry into the elastic-plastic stage is delayed, the ductility performance weakens, and the ability to withstand deformation decreases. The adopted composite form exhibits minimal relative slip at the interface, indicating good overall performance. Overall, the performance of the composite beams is optimal when the ratio of wood board thickness to steel I-beam height is 0.25 times.

Keywords

Wood-steel Composite I-beam; Thickness-to-height Ratio; Mechanical Properties; Model Test; Ultimate Bearing Capacity.

1. Introduction

In the current era of advancing modernization construction and rapid development of prefabricated structures, the combination of wood and steel, with their strong assembly advantages, significantly increases construction speed and reduces construction time. Therefore, wood and steel have become ideal materials for prefabricated structures.

Currently, domestic and foreign scholars have conducted a series of research on the combination forms and mechanical properties of wood-steel composite components, obtaining certain research results. Wang [1]et al. conducted a comparative study on the flexural performance of wood-steel composite I-beams and glued laminated timber I-beams. The results showed that the bending performance of composite beams, including ultimate bearing capacity, deformation capacity, maximum tensile and compressive strains along the grain, was much higher than that of glued laminated timber I-beams. Moreover, brittle shear failure of the timber flange along the grain direction was avoided. Duan [2]et al. studied the flexural performance of two groups of H-shaped wood-steel composite structures (with different connection or combination methods) and one group of pure steel structures. The experiments revealed that adding wood boards on both sides of the steel beam web could enhance the stability of the beam, and the steel web could provide sufficient shear stiffness, thus increasing the load-carrying capacity. Chen Aijun [3,4]et al. studied the flexural performance of steel flitch plates bolted together, finding that the arrangement of bolts in parallel or staggered and whether the two sections of the jointed beam come from the same glued laminated timber had little effect on the bending performance of the specimens. Prefabricated wood structures can use steel flitch plates bolted connections for longitudinal extension. Increasing the bolt end distance, diameter, and the thickness of both steel flitch plates and glued laminated timber can enhance the flexural bearing capacity of the steel flitch plate bolted connection node, but the degree of improvement gradually decreases beyond a certain range. Liu Degui [5]et al. conducted static bending tests on wood-steel composite beams to efficiently combine steel and wood and enhance flexural performance. They summarized the strengths of the influences of some relevant parameter factors on bending performance and proposed rational formulas for calculating the deflection and flexural bearing capacity of internally bonded thin-walled H-shaped wood-steel composite beams. Hassanieh [6]conducted four-point bending tests on wood-steel composite beams, analyzing load-deflection responses, short-term stiffness, and peak bearing capacity. The results showed that bolted composite beams significantly improved the stiffness and strength of the STC connection, and the combined use of adhesive mechanical connectors could provide almost complete composite action in STC beams, significantly increasing the initial stiffness of STC connections and beams. The degree of composite action to some extent affected the ultimate bearing capacity of STC beams.

In summary, domestic and foreign scholars have conducted research on various bending performance aspects of wood-steel composite beams, including combination forms, connectors, and cross-sectional geometric dimensions, yielding valuable results. However, there hasn't been research specifically on the influence of variations in specific cross-sectional geometric parameters on the mechanical properties of wood-steel composite beams with small shear span ratios. Therefore, based on the characteristics of high tensile strength and compressive strength along the grain for wood and high shear strength for steel, this paper designs wood-steel composite I-beams with small shear span ratios, where wood boards are bolted to the upper and lower flanges of steel I-beams. Through model tests, the paper aims to explore the influence of thickness-to-height ratio variations on the mechanical properties of wood-steel composite beams, providing a reference basis for future research and design of wood-steel composite beams.

2. Experimental Preparation and Implementation

2.1 Specimen Design

In order to investigate the influence of variations in the thickness-to-height ratio of wood boards on the mechanical properties of wood-steel composite I-beams, while controlling the span, section height, shear span ratio [7], and bolt arrangement, only the parameter of thickness-to-height ratio was changed. All beam components have a length of 750mm, a section height of 150mm, a section width of 145mm, and a shear span ratio of 2. The thicknesses of the wood boards for Groups L1 to L3 of the composite beams are 25mm, 35mm, and 45mm, respectively, with corresponding thickness-to-height ratios of 0.25, 0.44, and 0.75. Detailed parameters of the specimens for Groups L1 to L3 are shown in Table 1.

ISSN: 2414-1895 DOI: 10.6919/ICJE.202405_10(5).0057

Table 1. Main parameters of the specimens (unit: mm)

Specimen number	t_f	t_w	b_t	h_f	h_s	b_f	b	t	h	t/h_f	L	L_0	Longitudinal stiffeners
L1-1	3	4	-	94	100	130	145	25	150	0.25	750	600	Yes
L1-2	3	4	-	94	100	130	145	25	150	0.25	750	600	No
L2	3	4	-	74	80	130	145	35	150	0.44	750	600	No
L3	3	4	-	54	60	130	145	45	150	0.75	750	600	No

Note: tf, tw, hf, hs, and bf respectively refer to the flange thickness, web thickness, web height, overall height, and flange width of the I-beam; t and b respectively refer to the thickness and width of the wooden wing plate of the specimen; h, L, and L0 respectively refer to the total height, length, and calculated span of the composite beam and glued laminated timber beam; bt and t/hf respectively refer to the web width of the glued laminated timber beam and the thickness-to-height ratio of the composite beam.

2.2 Loading Scheme and Measurement Point Arrangement

This experiment adopts the method of concentrated loading at mid-span, referring to the “Standard for Test Methods of Wood Structures” (GB/T 50329—2012) [8]. To eliminate experimental system errors and ensure the normal operation of instruments and equipment, before formal loading, preloading is carried out to 20% of the estimated ultimate bearing capacity to check whether the instruments are working properly and to record the accuracy of the equipment. During formal loading, a step-by-step loading method is adopted: from 0 to 45 kN, each load is maintained at 5 kN for 1 minute; from 45 kN to 0.9 times the ultimate load, each load is 3 kN and maintained for 30 seconds; approaching the ultimate load, each load is 1 kN and maintained for 15 seconds; the test is stopped when significant damage occurs during the test or when the applied load drops suddenly to 80% of the bearing capacity.

The loading device used a 100-ton reaction frame and a 30-ton hydraulic jack. DH3861 static strain acquisition system and displacement meters were used to measure the strain and displacement of the specimens during loading, respectively. The arrangement of displacement meters for composite beams is shown in Fig. 1 (b).

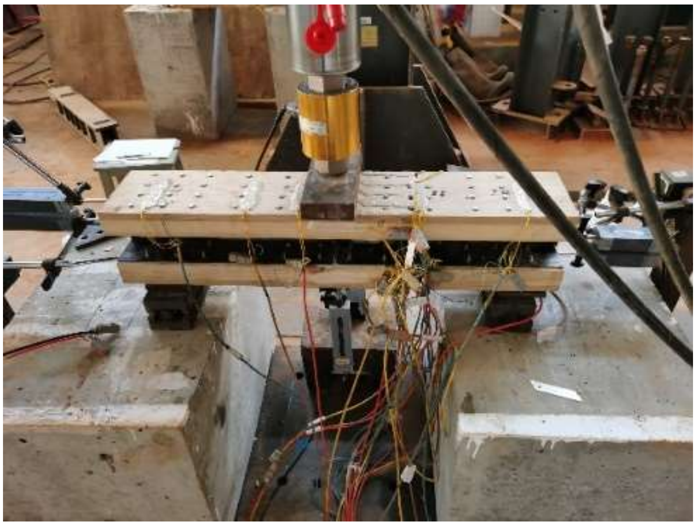

(a) Composite beam test loading device

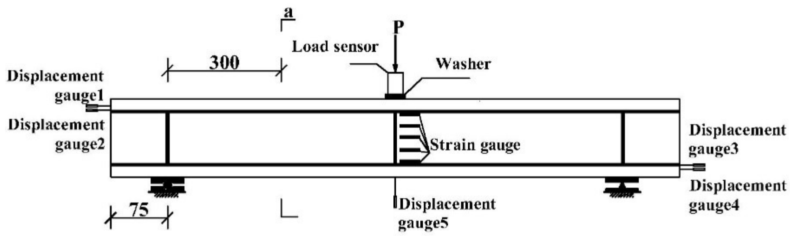

(b) Loading device and strain gauge arrangement for wood-steel composite beams (elevation)

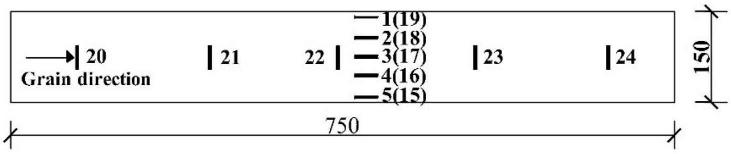

(c) Arrangement of strain gauges on the top surface of composite beam wood panels

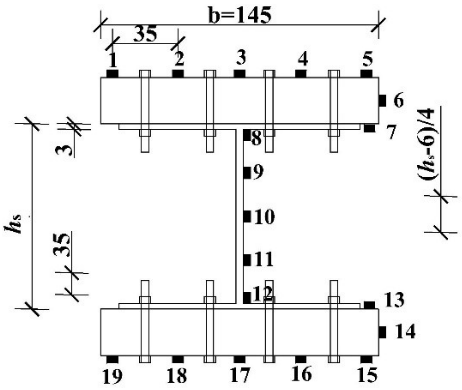

(d) Arrangement of strain gauge measurement points at mid-span section

Fig. 1 Experimental loading device, displacement meter, and strain measurement point arrangement (unit: mm)

3. Experimental Results Analysis and Discussion

3.1 Load-Deflection Analysis

The load-deflection curves of each specimen are shown in Fig. 2. The initial elastic stage slopes of the L2 and L3 groups of specimens are roughly the same, while for the L1-1 group, due to excessive stress concentration caused by too thin shims, there is a difference in the slope of the elastic stage compared to the L1 group. However, all composite beam components exhibit an ideal elastic-plastic form.

Stiffness is one of the most important performance indicators of specimens. The initial stiffness of the specimen can be obtained by the method proposed by Yasumura et al. [9], which defines the initial stiffness as the slope of the line connecting points $0.1P_{\max}$ and $0.4P_{\max}$. The initial stiffness of the specimen obtained using this method is shown in the table2.

According to the definitions of yield strength and yield point by Feng Peng [10]and Park R [11], this paper defines the yield displacement using the energy method as shown in Fig. 3 and quantifies the ductility performance using the deformation ductility coefficient λ, calculated by the following formula:

$$\lambda = \frac{\Delta_u}{\Delta_y} \tag{1}$$

In the equation: P_u-stands for ultimate load;

Δ_u -stands for corresponding deflection , i.e., ultimate displacement;

P_y-stands for yield load;

Δ_y -stands for corresponding deflection, i.e., yield displacement.

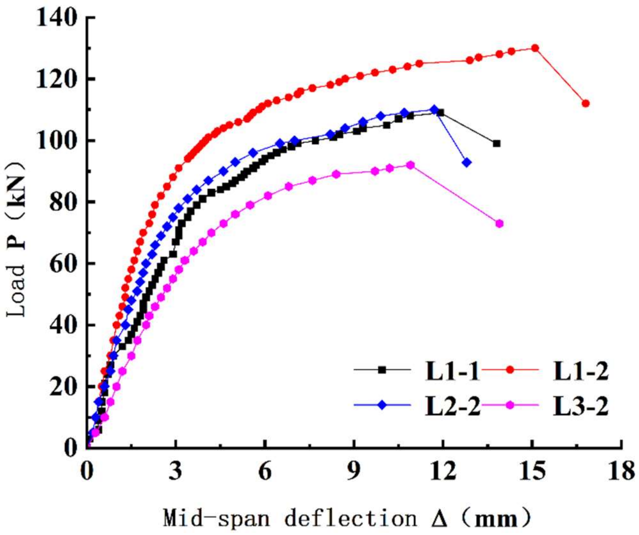

Fig. 2 Load-deflection curves

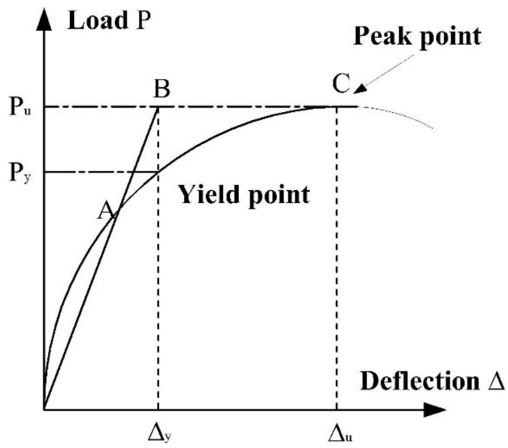

Fig. 3 Energy method

Table 2 presents the experimental results of various mechanical performance indicators for each specimen.

Table 2. Main mechanical performance indicators of specimens

Specimen number	P_u (kN)	Δ_u (mm)	P_y (kN)	Δ_y (mm)	Initial stiffness (kN/mm)	λ	$\overline{P_u}$ (kN)	$\overline{\lambda}$
L1-1	109	11.9	94.2	6.04	24.2	1.97	119.5	2.26
L1-2	130	15.1	111.3	5.92	41.1	2.55		
L2	110	11.7	94.8	5.33	30.6	2.20	110	2.2
L3	92	10.9	80.6	5.86	21.2	1,86	92	1.86

Note: $\overline{P_u}$ is the average value of the ultimate bearing capacity for each group, $\overline{\lambda}$ is the average value of the ductility coefficient for each group.

From Table 2, it can be seen that for the 3 groups of wood-steel composite beams, the L1 group has the highest ultimate bearing capacity, followed by the L2 group, and the L3 group has the smallest. Compared to the L2 group, the ultimate bearing capacity of the L1 group increased by 8.6%, and compared to the L3 group, it increased by 29.9%. The deformation of the L1 group is also the most obvious, indicating that the combination ratio of the L1 group specimens can better leverage the strength advantages of the two materials.

For the initial stiffness of the specimens, as the thickness-to-height ratio increases, the initial stiffness decreases. For the same thickness-to-height ratio composite beam, installing longitudinal stiffeners significantly increases the initial stiffness compared to specimens without longitudinal stiffeners, indicating that specimens with a smaller thickness-to-height ratio have stronger resistance to deformation in the early stages of loading, and longitudinal stiffeners can effectively increase the stiffness of composite beams, improving the overall specimen's resistance to deformation.

For the ductility performance of composite beams, the ductility coefficient of the L1 group specimens is 5.1% higher than that of the L2 group, and the L2 group is 18.1% higher than the L3 group, indicating that the higher the proportion of wood, the later the entry into the plastic stage, and the weaker the ductility performance, the weaker the ability to withstand deformation. In addition, as the

ISSN: 2414-1895 DOI: 10.6919/ICJE.202405_10(5).0057

thickness-to-height ratio increases, the ductility performance of composite beam specimens decreases, and the ability to withstand non-elastic deformation weakens accordingly.

3.2 Load-Slip Response

When the shear force at the interface of composite beams exceeds the friction force during loading, certain deformations occur in the bolts due to the longitudinal shear force at the interface. Additionally, during component fabrication, the pre-drilled holes for bolts are slightly larger than the bolt diameter for ease of installation. Furthermore, due to differences in hardness between steel and wood, variations exist in the deformation degree of the steel and wood in contact with the bolt. All these factors eventually lead to relative sliding at the wood-steel interface, reducing the composite efficiency of the beams and consequently decreasing the load-bearing capacity of the composite components. In this experiment, under the action of concentrated load at mid-span, deflection occurred at the mid-span of the beam, and relative sliding at the interfaces at both ends as shown in Fig. 4 happened. The relative sliding of the lower wing timber relative to the I-beam protrudes outward, and the relative sliding δ_1 is positive numbers; The upper wing timber relative to the I-beam shrinks inward, and the relative sliding δ_2 is negative numbers.

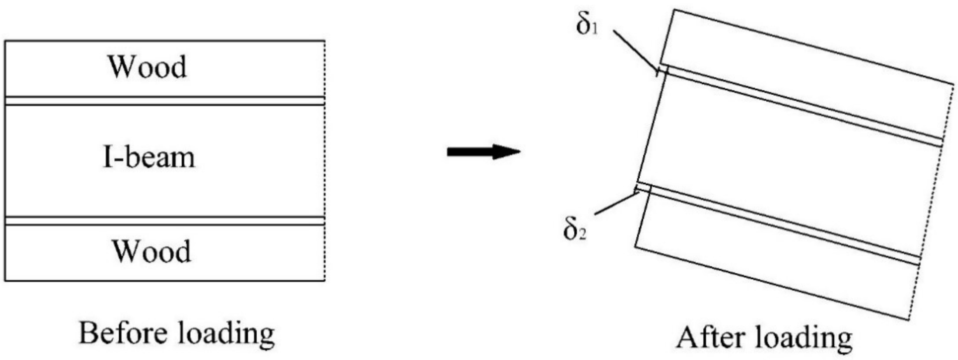

Fig. 4 Load slip diagram

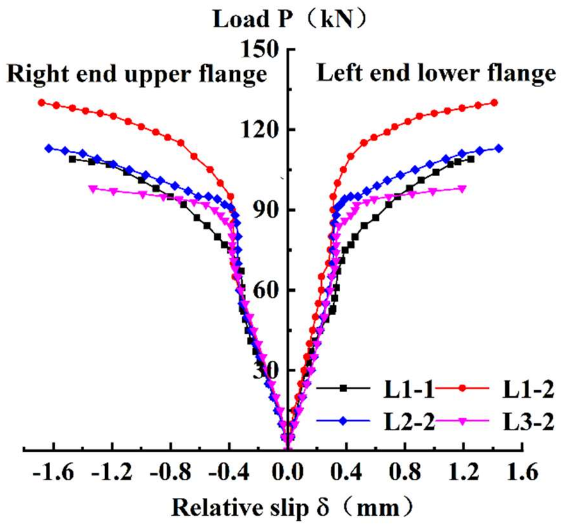

Fig. 5 Relative slip of composite beam

The results of the slip test are shown in Fig. 5 and Table 3. The relative slip of each group of components increases with the increase of load. Initially, the relative slip increases linearly with the load. When the relative slip reaches a certain value, the rate of increase in relative slip with load decreases. However, it quickly increases again later. This is because during specimen fabrication, the pre-drilled bolt holes are slightly larger than the bolts for ease of installation, resulting in gaps between the bolts and the wood and I-beams. When sliding to a certain extent, resistance occurs when the bolt contacts the hole wall of the I-beam and timber, which slows down the rate of relative sliding. Subsequently, with the increase of load, the bolts deform due to the large shear stress, and the relative sliding at the interface between the two begins to increase rapidly again. From Table 3, it can be seen that the maximum slip of the upper and lower flanges of the composite I-beam is 1.68mm. This indicates that the slip of such components is relatively small, and the bolt arrangement is reasonable, which greatly reduces the impact of relative sliding on the ultimate bearing capacity of the components.

Table 3. Relative slip of composite beam interface (mm)

Specimen number	$\delta_{1\max}$	$\delta_{2\max}$
L1-1	1.25	-1.47
L1-2	1.41	-1.68
L2	1.44	-1.63
L3	1.19	-1.33

Note: $\delta_{1\max}$ is the maximum relative slip value of the lower flange on the right end (bottom timber protruding outward from the I-beam); $\delta_{2\max}$ is the maximum relative slip value of the upper flange on the left end (top timber shrinking inward from the I-beam).

4. Conclusion

(1) In the three groups of wood-steel composite I-beams, the lower flange timber of all three groups finally failed due to tension, and different degrees of grain splitting occurred on the upper flange boards of all three groups of specimens. In the composite beams with a thickness-to-height ratio of 0.25, no local buckling of the upper flange of the I-beam occurred without longitudinal stiffening ribs. Other thickness-to-height ratios with or without stiffening ribs did not exhibit this phenomenon, indicating that different thickness-to-height ratios affect local failure phenomena, and longitudinal stiffening ribs can effectively prevent local buckling of the upper flange of the I-beam.

(2) With the increase of thickness-to-height ratio, the ultimate bearing capacity of the composite beam decreases. The ultimate bearing capacity of the composite beam with a thickness-to-height ratio of 0.25 is higher than that of the composite beams with thickness-to-height ratios of 0.44 and 0.75. Compared with group L2, the ultimate bearing capacity of group L1 increased by 8.6%, and compared with group L3, it increased by 29.9%. The deformation of group L1 specimens is also the most obvious; the ductility coefficient of group L1 specimens is 5.1% higher than that of group L2 specimens, and 18.1% higher than that of group L3 specimens; the higher the thickness-to-height ratio, the later it enters the elastic-plastic stage, the weaker the ductility, and the weaker the ability to withstand deformation. It shows that the ratio of wood board thickness to I-beam height of 0.25 is more favorable for improving the shear resistance of the beam.

References

[1] Wang J, Lu Y, Lei Y, et al. Comparative Study on Flexural Behavior of Steel-Timber Composite beams and Glued Timber I-Beams[J]. Journal of Engineering Science & Technology Review, 2020, 13(6).

[2] Duan S, Zhou W, Liu X, et al. Experimental study on the bending behavior of steel-wood composite beams[J]. Advances in Civil Engineering, 2021, 2021: 1-12.

[3] Aijun Chen, Dong Niu, Zhifeng Wang, Jiejun Wang. Experimental Study on Bending Resistance of Glued Laminated Timber Beams with Steel Plate-Bolt Connections[J]. Highway Engineering, 2020, 45(06): 15-21+26. DOI: 10.19782/j.cnki.1674-0610.2020.06.003.

[4] Aijun Chen, Runbo Peng, Guojing He, Haolei Wang, Jiejun Wang. Study on Bending Resistance of Glued Laminated Timber Beams with Steel Plate-Bolt Connections[J]. Journal of Railway Science and Engineering, 2022, 19(02): 500-510. DOI: 10.19713/j.cnki.43-1423/u.t20210165.

[5] Degui Liu, Yuhao Wang, Yong Wen, Wei Zou, Tao Wang. Study on Bending Performance of Embedded Thin-walled H-section Steel-Timber Composite Beams[J]. Journal of Building Structures, 2022, 43(05): 149-163. DOI: 10.14006/j.jzjgxb.2020.0593.

[6] Hassanieh A, Valipour H R, Bradford M A. Experimental and numerical study of steel-timber composite (STC) beams[J]. Journal of Constructional Steel Research, 2016, 122: 367-378.

[7] Lei Cao, Bowang Chen. Review on Shear Performance of Glued Laminated Timber Beams[J]. Engineering Mechanics, 2018, 35(06): 1-5+14.

[8] Ministry of Housing and Urban-Rural Development of the People's Republic of China. Testing Methods for Timber Structures GB50329-2002[S]. Beijing, 2002.

[9] Estimating seismic performance of wood-framed structures[C/CD]. Yasumura M,Kawai N. Proceedings of 1998 IWEC . 1998.

[10] Peng Feng, Hanlin Qiang, Lieping Ye. Definition and Discussion on "Yield Point" of Materials, Components, and Structures[J]. Engineering Mechanics, 2017, 34(03): 36-46.

[11] Park R. State of the art report ductility evaluation from laboratory and analytical testing [C]. Proceedings of.